Global Biogeochemical Cycles

Supporting Information for

Rapid expansion of fixed nitrogen deficit in the eastern Pacific Ocean revealed by 50-year time series

Natalya Evans[1], Juliana Tichota[1], Wendi Ruef[2], James Moffett[1], and Allan Devol[2]*

[1]Department of Biological Sciences, University of Southern California; Los Angeles, California.

[2]School of Oceanography, University of Washington; Seattle, Washington.

Contents of this file

Introduction

Additional information about the methods used for integration, water mass analysis, time series comparison, and natural variability estimation are provided in this document. Additional figures and tables provide visualizations and additional statistical information supporting the methods described in the manuscript as well as this Supplemental Information.

Text S1. Water mass analysis

Conservative temperature and absolute salinity were used rather than *in situ* measurements because they are more conservative across wider areas, such as on the shelf (Evans, Boles, et al., 2020). Oxygen was not used in this eOMP because within the ODZ, oxygen concentrations are below the detection limit of conventional instrumentation, such as SBE43 sensors (Revsbech et al., 2009), and report wide-ranging concentrations. Therefore, oxygen cannot be implemented in the ETNP ODZ to compare between cruises, which was a primary goal for this project. SiO_4^{2-} was included in this paper but not Evans et al. (2020) due to data availability. Evans et al. (2020) also used spiciness as a proxy for dissolved oxygen because these two parameters are hydrographically correlated in the California Current System. As Evans et al. (2020) established that these water masses are coherent on potential density surfaces and oxygen was not used in this eOMP, potential density replaced spiciness. Potential density has previously been used in other OMPs (Jenkins et al., 2015). Due to the recent development of a Python optimum multiparameter analysis package that allows for flexible constraints and underconstrained solutions (Shrikumar et al., 2022), we recommend that future scientists performing water mass analysis use this package rather than the MATLAB omp2 package, and we may also use it to re-process this data ourselves. Slight differences in the endmembers in eOMP for the ETNP ODZ on the 110 ºW exist between our formulation in the Matlab omp2 package and the pyompa package due to the addition of multiple, flexible respiration pathways in pyompa.

After the ideal eOMP settings were selected, eOMP was performed on each cruise individually with the same basis to prevent any outliers in the data from one cruise from influencing another. This step was performed because the eOMP calculation standardizes the input data. We applied eOMP between potential densities of 24.75 kg m^{-3} to 27.2 kg m^{-3} to match the integrations, however, our basis set was built for 26 kg m^{-3} to 27 kg m^{-3} to limit the inclusion of thermocline water masses in the eOMP. Our results converge best within 26 kg m^{-3} to 27 kg m^{-3}, and we caution users from using the results outside this range without scrutiny.

In most eOMP calculations, ΔP represents aerobic remineralization processes (Karstensen & Tomczak, 1998). To prevent confusion, we use ξ to represent the accumulated anaerobic remineralization. This choice of symbol is partially motivated because ξ is canonically used to represent the extent of reaction in physical chemistry(Ontiveros-Cuadras et al., 2019). This mathematics representing the use of ξ are presented in Eq. 1. The water type definitions used for quantifying water mass content are presented in Table S4. The eOMP package developed by Karstensen and Tomczak solves a linear system of equations for every sample. This system of equations is represented in general in Eq. 2, where A is the water types, x is the water mass content being solved for, and b is the measured data. Eq. 3 provides a more detailed depiction of how this paper calculated water mass content, including the residuals for each fit. Within the eOMP calculation, each parameter in Eq. 4 is standardized then weighted, but this step is not presented below for clarity. eOMP-derived fixed nitrogen loss was calculated

by multiplying ξ by 62, and the maximum fixed nitrogen loss was calculated by taking the mean of values greater than the 90% quantile for fixed nitrogen loss for each cruise. The difference between N* and 62ξ is presented in Fig. S3. For researchers interested in the relationships between these calculations, we fit N* to 62ξ using a Type 2 linear regression for values within potential densities of 26.2 kg m^{-3} to 26.8 kg m^{-3} and display the results in Eq. 4.

$$[PO_4^{3-}] = [PO_4^{3-}]_o + \xi \quad (1)$$

$$Ax - b = 0 \quad (2)$$

$$\begin{bmatrix} \theta_{ESW} & \theta_{13CW} & \theta_{NEPIW} & \theta_{AAIW} & \theta_{uPSUW} & 0 \\ S_{A,ESW} & S_{A,13CW} & S_{A,NEPIW} & S_{A,AAIW} & S_{A,uPSUW} & 0 \\ [PO_4]_{ESW} & [PO_4]_{13CW} & [PO_4]_{NEPIW} & [PO_4]_{AAIW} & [PO_4]_{uPSUW} & 1 \\ [NO_3]_{ESW} & [NO_3]_{13CW} & [NO_3]_{NEPIW} & [NO_3]_{AAIW} & [NO_3]_{uPSUW} & -62 \\ [SiO_4]_{ESW} & [SiO_4]_{13CW} & [SiO_4]_{NEPIW} & [SiO_4]_{AAIW} & [SiO_4]_{uPSUW} & 11.4 \\ \sigma_{\theta,ESW} & \sigma_{\theta,13CW} & \sigma_{\theta,NEPIW} & \sigma_{\theta,AAIW} & \sigma_{\theta,uPSUW} & 0 \end{bmatrix} \begin{bmatrix} x_{ESW} \\ x_{13CW} \\ x_{NEPIW} \\ x_{AAIW} \\ x_{uPSUW} \\ \xi \end{bmatrix} - \begin{bmatrix} \theta_{obs} \\ S_{A,obs} \\ [PO_4]_{obs} \\ [NO_3]_{obs} \\ [SiO_4]_{obs} \\ \sigma_{\theta,obs} \end{bmatrix} = \begin{bmatrix} \varepsilon_\theta \\ \varepsilon_{S_A} \\ \varepsilon_{PO_4} \\ \varepsilon_{NO_3} \\ \varepsilon_{SiO_4} \\ \varepsilon_{\sigma_\theta} \end{bmatrix} \quad (3)$$

$$62\xi = (0.883 \pm 0.026)N^* - (3.82 \pm 0.11) \quad (4)$$

We plotted the Bograd et al. (2019) Pacific Equatorial Water definitions as a helpful comparison for analyzing water masses in the eastern Pacific. uPEW and dPEW are synonymous with 13CW and NEPIW, appropriately (Evans, Schroeder, et al., 2020), but Bograd et al. (2019) defined their PEW water masses more to the southwest than the repeat hydrographic line this study focused on. In the ETNP below the thermocline, salinity slightly increases with eastward transit, as observed in longitudinal transects through the ETNP ODZ (Evans, Boles, et al., 2020). Therefore, the small shift in absolute salinity between the 13CW and NEPIW versus the uPEW and dPEW is not surprising, and it appears larger when plotted using practical salinity. The 13CW and uPEW are offset on the NO_3^--PO_4^{3-} plot, suggesting that noticeable aerobic remineralization occurs between where Bograd et al. (2019) defines their PEW water types and this sample location. This deviation fits the flow path of these water masses based on where they enter the ETNP ODZ and the remineralization that occurs as they transit (Evans et al., 2022). In the SiO_4^{2-}-PO_4^{3-} plot, the 13CW, NEPIW, and uPSUW water mass definition SiO_4^{2-}values are lowered to minimize residuals of fit.

Year	R/V	Start month	Cruise ID
1972	*Thomas G. Thompson*	February	TGT66
1994	*Discoverer*	January	WOCE_P18
2007	*Ronald Brown*	December	P18_2007
2012	*Thomas G. Thompson*	March	TN278
2016	*Ron Brown*	November	P18_2016
2016	*Sikuliaq*	December	SKQ201617S
2018	*Roger Revelle*	March	RR1804
2019	*Kilo Moana*	September	KM1919

Table S1. Table listing each cruise and metadata about each cruise.

Cruise ID	NO_3^-/µmol kg^{-1}	PO_4^{3-}/µmol kg^{-1}
TGT66	1.006	1.043
WOCE_P18	0.999	0.998
P18_2007	1.009	0.992
TN278	1.014	**1.042**
P18_2016	1.009	1.013
SKQ201617S	**1.025**	**1.082**
RR1804	**1.056**	1.004
KM1919	**1.073**	1.019

Table S2. Table containing the GLODAP corrections for each cruise, where bolded values were applied as scaling factors to correct for systemic differences in measurement.

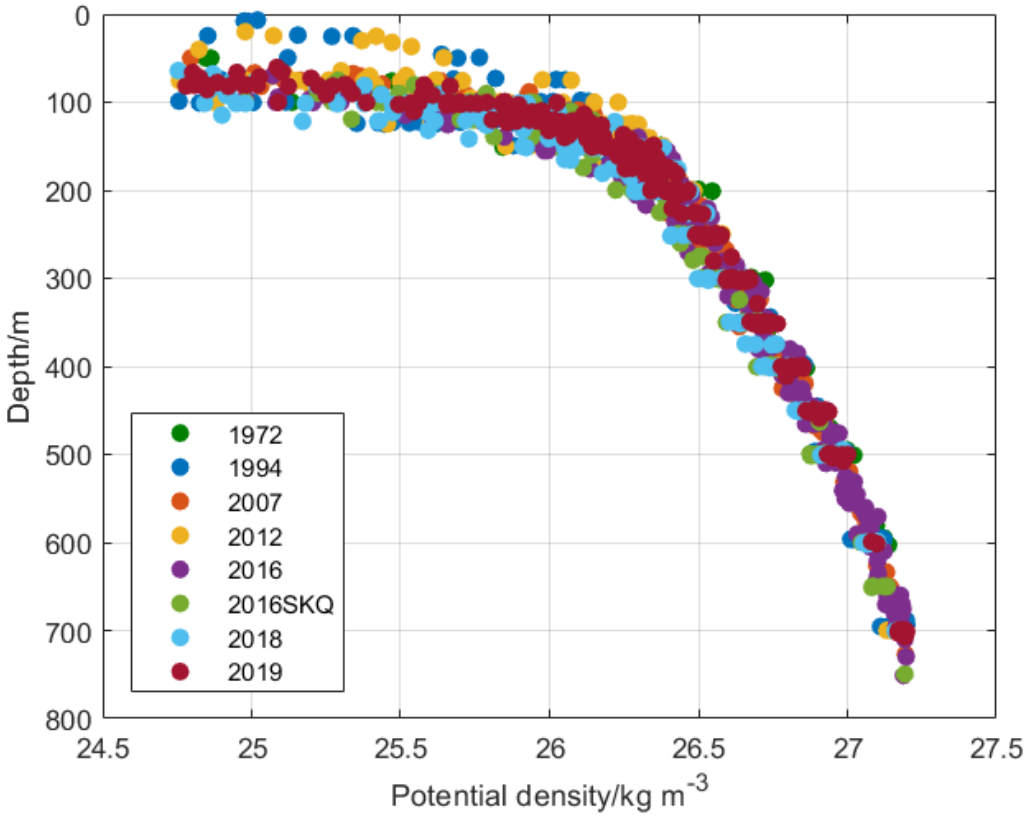

Figure S1. Scatter plot of data from each of the eight cruises in the ETNP ODZ depicting depth versus potential density.

	1972	1994	2007	2012	2016	2016SKQ	2018	2019
24.75-27.2 kg m^{-3}	6.63E6	6.55E6	6.93E6	7.43E6	7.41E6	7.79E6	7.58E6	8.44E6
24.75-26.2 kg m^{-3}	5.84E5	5.20E5	5.87E5	7.24E5	7.14E5	9.03E5	7.60E5	7.58E5
26.2-26.8 kg m^{-3}	2.97E6	2.78E6	3.18E6	3.56E6	3.39E6	3.60E6	3.46E6	3.77E6
26.8-27.2 kg m^{-3}	2.97E6	3.14E6	3.04E6	3.01E6	3.21E6	3.15E6	3.47E6	3.78E6

Table S3. This table presents the results from integrating fixed N loss, as seen in Fig. 4a-c, however, these data are not corrected with the 0.747 scaling factor that was applied for plotting them in Fig. 5a-c.

	ESW	13CW	NEPIW	AAIW	uPSUW	ξ	Weight
θ/ºC	23.28	13.41	9.47	5.53	7.75	n/a	16
S_A/g kg^{-1}	34.52	34.95	34.78	34.70	32.80	n/a	1
PO_4^{3-}/µmol kg^{-1}	0.17	2.33	2.65	3.27	1.13	1	4
NO_3^-/µmol kg^{-1}	0	29.99	35.60	44.80	10.08	-62	6
SiO_4^{2-}/µmol kg^{-1}	1.28	23.50	33.86	83.53	10.33	11.4	14
σ_θ/kg m^{-3}	23.30	26.29	26.74	27.25	25.6	n/a	16

Table S4. Water mass definitions used in extended optimum multiparameter analysis, including anaerobic remineralization and weighting for each parameter.

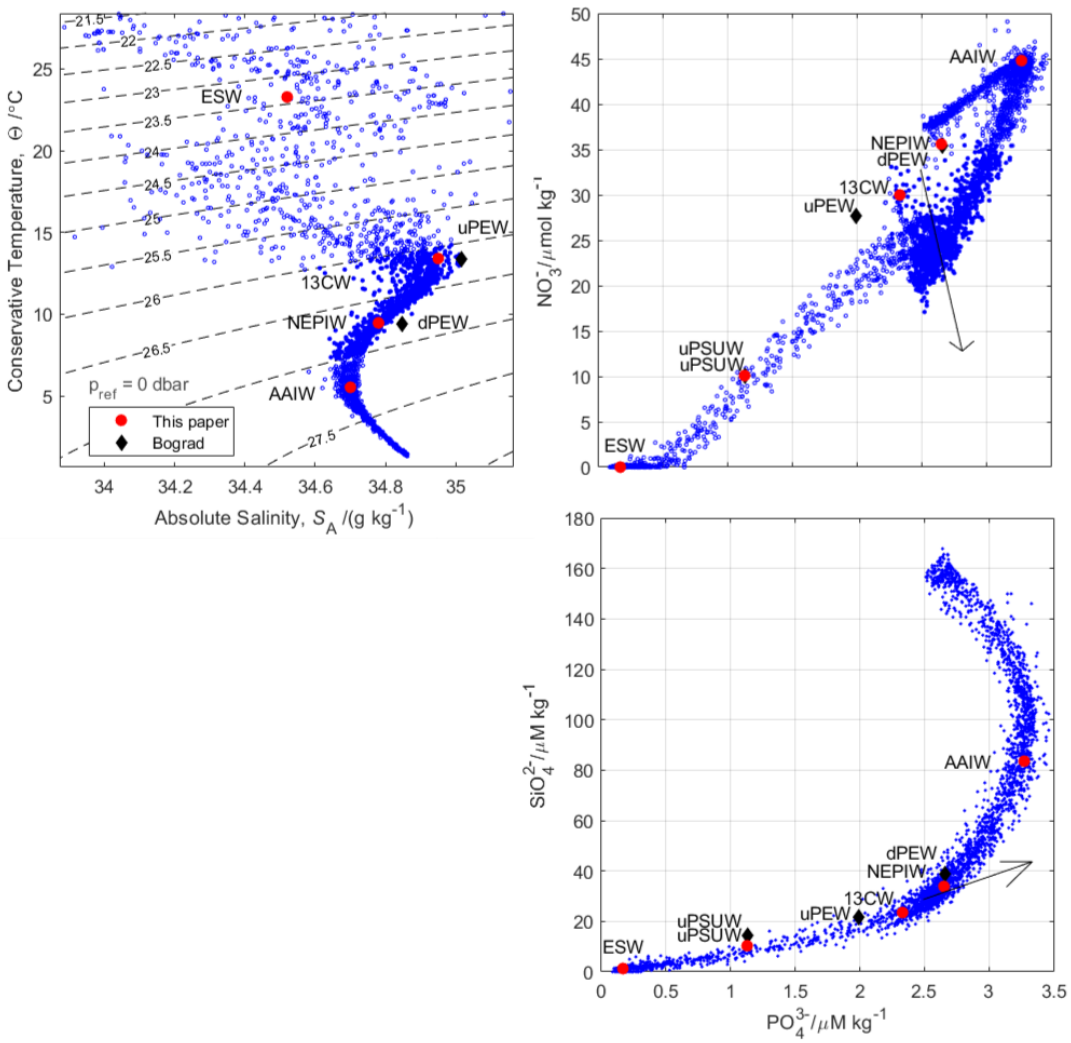

Figure S2. Water mass endmembers, in red diamonds as well as black circles for Bograd et al. (2019), superimposed over the input data to eOMP in blue.

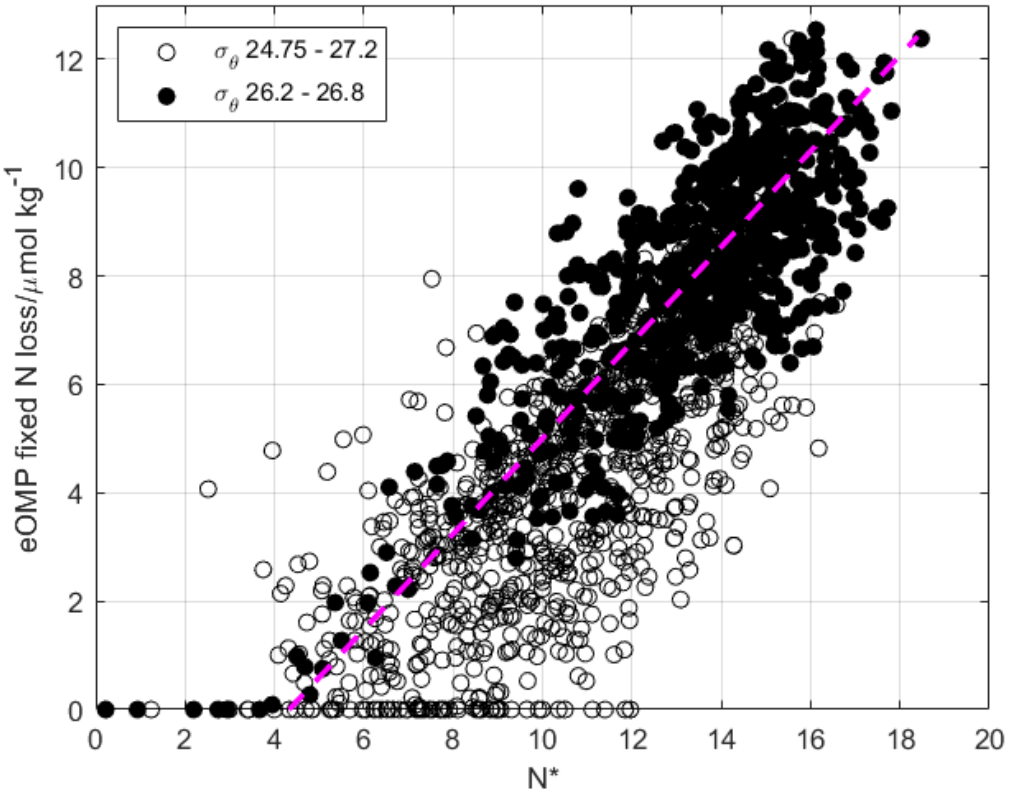

Figure S3. Comparison between N* and eOMP-derived fixed nitrogen loss, described previously as 62ξ.

	Parameter	1972	1994	2007	2012	2016	2016SKQ	2018	2019
26.2-26.8 kg m^{-3}	Mean	10.77	9.43	10.77	11.83	11.02	10.78	11.19	11.79
	Std	0.17	0.65	0.51	0.35	0.59	0.56	0.50	0.42
	n	3	10	9	11	7	7	11	13
26.8-27.2 kg m^{-3}	Mean	8.1	7.92	7.72	7.23	7.29	8.12	8.7	9.74
	Std	1.0	0.44	0.60	0.16	0.67	0.25	1.4	0.48
	n	3	7	6	4	7	2	7	7

Table S5. Mean fixed N loss data, calculated via eOMP, as depicted in Fig. 6a..

	O_2/μM					
Year	Winter	Spring	Summer	Fall	Mean	Standard deviation
1984	83	78	76	74	78	4
1985	68	68	72	71	70	2
1986	78	75	67	86	76	8
1987	86	88	86	87	87	1
1988	88	0	82	85	85	3
1989	79	78	81	91	82	6
1990	0	0	87	98	93	8
1991	95	0	92	90	92	2
1992	90	96	97	92	94	3
1993	98	97	96	99	97	1
1994	102	96	82	95	94	8
1995	102	87	95	87	93	7
1996	92	93	86	87	89	3
1997	88	87	85	74	83	6
1998	99	97	96	0	97	1
1999	88	86	85	87	86	1
2000	86	84	83	84	84	1
2001	87	85	83	86	85	2
2002	85	82	79	83	82	2
2003	84	79	68	80	78	7
2004	84	82	78	82	81	2
2005	82	81	78	71	78	5
2006	77	76	74	79	77	2
2007	80	77	78	70	76	4
2008	72	73	77	77	75	3
2009	75	79	73	82	77	4
2010	87	77	76	71	78	7
2011	77	70	73	73	73	3
2012	70	54	66	74	66	8
2013	75	65	73	77	73	5
2014	42	71	83	84	70	20
2015	0	76	76	76	76	0
2016	86	78	70	80	78	7
2017	81	76	76	80	78	2
2018	0	82	80	82	82	1
2019	0	72	73	81	75	5

Table S6. Mean oxygen concentrations measured on CalCOFI cruises, by each season and year, then the means and standard deviations used in Fig. 6b.

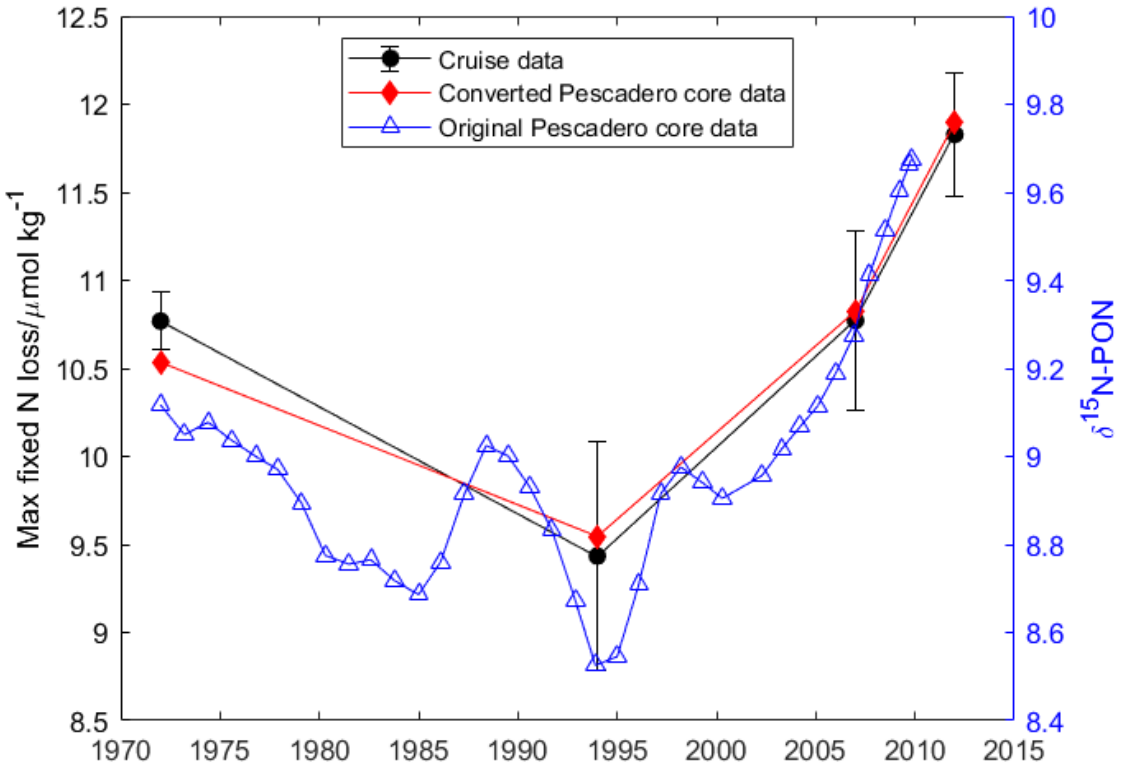

Figure S4. Plot highlighting the four maximum fixed N loss measurements from eOMP calculations (black circles) versus the "rloess" Pescadero basin N isotope data, on the right y-axis, used for conversion. We also display this Pescadero basin data converted to max fixed N loss using m=1.68±0.19 and b=-4.8±1.8 with Eq. 4.

	1972	1994	2007	2012	2016	2016SKQ	2018	2019
Mean	152.1	122.1	119.0	136.6	138.5	147.4	127.2	152.1
Standard deviation	0.76	0.47	1.3	0.52	0.64	1.1	1.7	0.76
Number of samples	11	10	11	11	7	11	11	11

Table S7. Depth of the 13CW water depicted in Fig. 6a, with the number of samples with 13CW as determined from 1-m binned data, the mean depth, and the standard deviation.

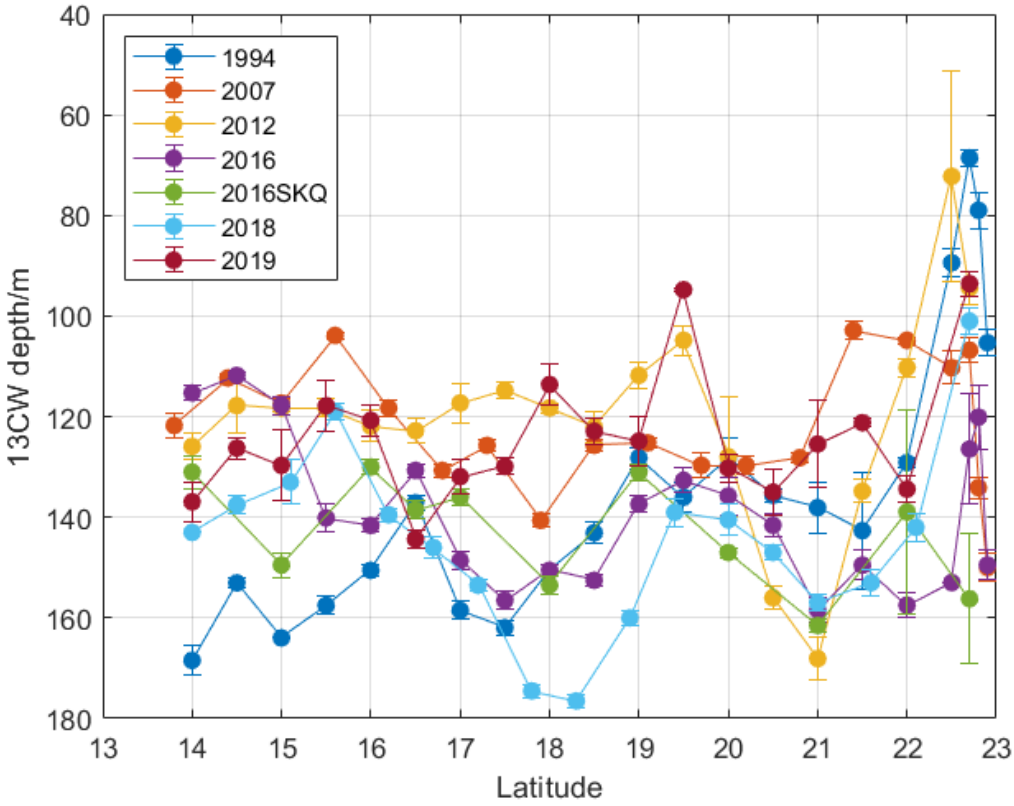

Figure S5. Depth of the 13CW for each station on each expedition. Data between 14 and 19 ºN is used to generate the data in Table S6..

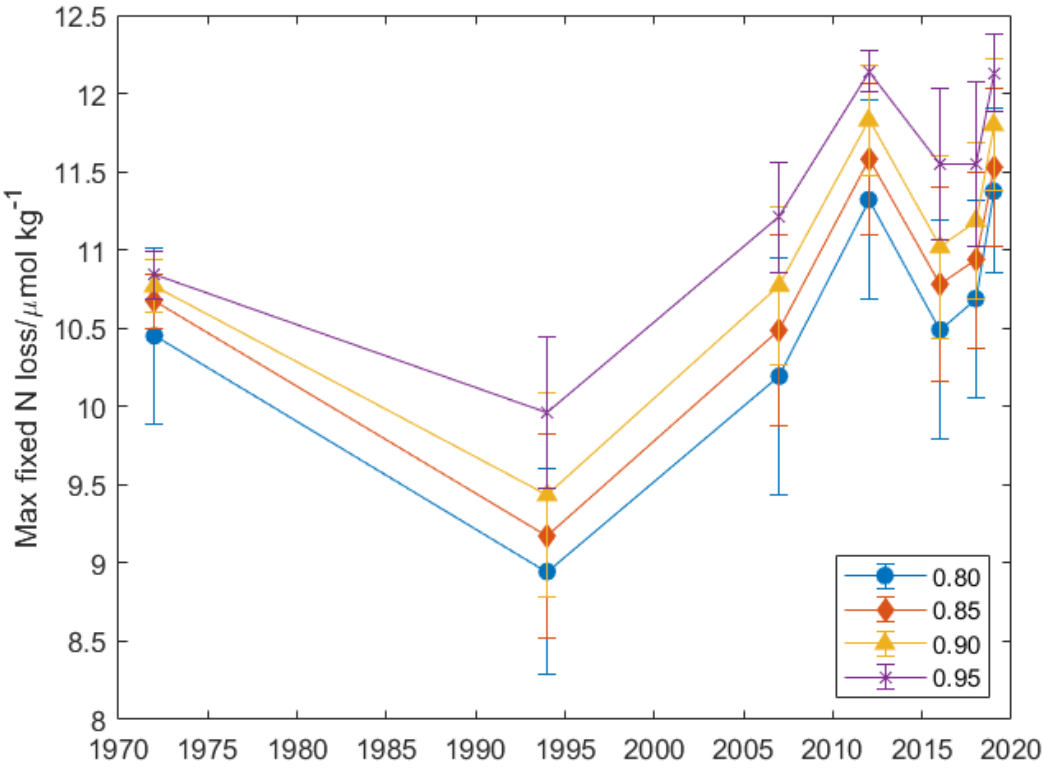

Figure S6. Sensitivity analysis for calculating the strength of the core ETNP ODZ based on quantile. The mean and standard deviation for the 80%, 85%, 90%, and 95% quantile are presented.